Applied Thermal Engineering 219 (2023) 119643

Contents lists available at ScienceDirect

Applied Thermal Engineering

journal homepage: www.elsevier.com/locate/apthermeng

Research Paper

The effect of partial loads on the performance of a funnel solar cooker

Xabier Apaolaza-Pagoaga [a,*], Antonio Carrillo-Andrés [a], Celestino Rodrigues Ruivo [b,c], Francisco Fernández-Hernández [a]

[a] Energy Research Group. Department of Mechanical, Thermal and Fluids Engineering, University of Malaga, Calle Arquitecto Francisco Peñalosa, 6, 29071 Malaga, Spain
[b] Department of Mechanical Engineering, Institute of Engineering, University of Algarve, Campus da Penha, 8005-139 Faro, Portugal
[c] ADAI - LAETA, Rua Pedro Hispano nº 12, 3030-289 Coimbra, Portugal

ARTICLE INFO

Keywords:
Funnel solar cooker
Partial load
Experimental study
Performance evaluation

ABSTRACT

Several solar cooker designs have been proposed over the last decades. The funnel cooker is a well-known model, representative of the category of panel-type solar cookers. From the empirical experience of real practice, it is known that the use of partial loads has an impact on the performance of the cooker. However, this effect has not yet been investigated rigorously. This work aims to fill this lack. Extensive experimental work was performed to determine the effect of partial loads on a funnel cooker thermal performance. Tests were conducted on two identical funnel cookers, in Malaga, Spain, with low sun elevation. Cookers were tracked only azimuthally. Experimental protocol was based on ASAE 580.1 Standard for better replicability. Results showed that the standardised power drops by about 15% of the original value when the water volumetric load fraction drops by 25%, for both cooker operations, with and without glass enclosure. This important reduction is explained on how the fill level of the cooking vessel affects its function as a thermal radiation receiver. Results from experimental tests were correlated into a simple formula of practical interest. Finally, a new cooking vessel design, that improves performance at partial loads, i.e., a 25.4% increase in cooker power, was proposed and tested.

1. Introduction

Solar cookers are devices that use solar energy to heat, cook, or pasteurise food or drink. Solar cookers are useful tools in mitigating situations of energy poverty, which affects millions of human beings [1]. In addition, in industrialised countries, a larger-scale use of solar cooking would have a positive impact in reducing the carbon footprint [2]. Solar cookers are also excellent educational tools [3,4] and a valuable cooking option in some emergency situations such as natural disasters or power outages [5,6].

Over decades, many different solar cookers designs have evolved. Some comprehensive reviews can be found in literature [7–9,10]. Saxena et al. [10] have discussed on thermal and photovoltaic solar cooking systems giving attention to the associated social, cultural, and economic aspects. Most of today's solar cookers can be classified into four main categories: parabolic, panel, box, and tube cookers [11–13]. This work focuses on the performance of panel solar cookers, which are usually low-cost devices, without heat storage media, easy to build and often portable. They use various reflective panels to direct sunlight onto a cooking vessel, usually contained in an enclosure, made of clear plastic or glass. Solar panel cookers require little tracking of the sun and allow unattended cooking. More than 40 designs of panel solar cookers are available in open domain [14]. Some popular designs are the Cookit [15], HotPot [16], Haines [17,18], Copenhagen [19], and Funnel [20–23].

Solar cookers are essentially thermal machines, so their thermal performance is a key factor. It can be determined by analysis of optical and thermal characteristics of the cooker design or by experimental testing. There are several parameters commonly used for performance investigation of solar cooking systems [9], such as the figures of merit *F1* and *F2* [24], the opto-thermal ratio (*COR*) [25] or the standardised cooker power [26,27].

Several papers have recently appeared investigating different aspects that influence the thermal performance of solar panel cookers. In case of funnel type cookers, Ruivo et al. [20] experimentally found that adopting a glass lid for the cooking vessel increased the standardised cooker power [27] by 46% compared to the value when using an opaque black metal lid. Apaolaza-Pagoaga et al. [22] investigated the influence of changing the vertical position of the cooking vessel and determined the optimal trivet height to be 25 mm. Sagade et al. [21] studied the performance of funnel solar cookers at intermediate temperatures, i.e.,

* Corresponding author.

https://doi.org/10.1016/j.applthermaleng.2022.119643
Received 2 June 2022; Received in revised form 10 October 2022; Accepted 13 November 2022
Available online 20 November 2022

Nomenclature

A_c	Intercept area of the solar cooker (m^2)
A_r	Receiver area (m^2)
a	Slope of the linear regression of standardised power (W $°C^{-1}$)
C_g	Cooker geometric concentration ratio (-)
COR	Opto-thermal ratio (m^2 °C W^{-1})
c_w	Specific heat of water (J $°C^{-1}$ kg^{-1})
F'	Heat exchange efficiency factor (-)
$F1$	First figure of merit (W m^{-2} $°C^{-1}$)
$F2$	Second figure of merit (-)
h_w	Water line height (m)
I	Solar irradiance (W m^{-2})
I_{bn}	Beam normal solar irradiance (W m^{-2})
$\bar{I}_{bn}$	Average beam normal solar irradiance during a test (W m^{-2})
I_n	Global normal solar irradiance, i.e., global solar irradiance on plane perpendicular to beam radiation (W m^{-2})
$\bar{I}_n$	Average global normal solar irradiance during a test (W m^{-2})
LAR	Load-to-area ratio (kg m^{-2})
m_w	Mass of water (kg)
n_p	Number of valid observation points for deriving the linear regression
n_t	Number of tests
n_{t1}	Number of tests performed with cooker CSR1
n_{t2}	Number of tests performed with cooker CSR2
$\dot{Q}$	Cooker power (W)
$\dot{Q}_S$	Standardised cooker power (W)
$\dot{Q}_{S,0}$	Standardised cooker power for $\Delta T_{w,a} = 0$ °C (W)
$\dot{Q}_{S,50}$	Standardised cooker power for $\Delta T_{w,a} = 50$ °C (W)
$\dot{Q}_{S,CI95\%}$	95% confidence interval for the standardised power (W)
$\dot{Q}_{S,PI95\%}$	95% prediction interval for the standardised power (W)
$\dot{q}_{S,m,50}$	Standardised power per unit of mass load for $\Delta T_{w,a} = 50$ °C (W kg^{-1})
R^2	Coefficient of determination (-)
t	Time (s)
T_a	Ambient temperature (°C)
$\bar{T}_a$	Average ambient temperature during a test (°C)
T_w	Water temperature (°C)
U_L	Heat loss factor (W m^{-2} $°C^{-1}$)
v_a	Wind velocity (m s^{-1})
$\bar{v}_a$	Average wind velocity during a test (m s^{-1})
VLF	Volumetric load fraction (-)
V_{pot}	Volume of the cooking vessel or pot (m^3)
V_w	Volume of water load (m^3)

Greek symbols

α_s	Sun elevation angle (°).
$\bar{\alpha}_s$	Average sun elevation angle during a test (°)
Δt_i	Time interval (s) or (min)
$\Delta T_{w,i}$	Increase in water temperature for each time interval (°C)
$\Delta T_{w,a}$	Difference between water load and ambient temperature (°C)
η_0	Optical efficiency (-)
η	Efficiency (-)
ψ_{axis}	Elevation angle of the central axis of the solar cooker (°)

Subscripts

n	Direction normal to beam radiation
i	Time interval i

Abbreviations

CSR1	Funnel solar cooker number 1
CSR2	Funnel solar cooker number 2
HBW	Hottel-Whillier-Bliss

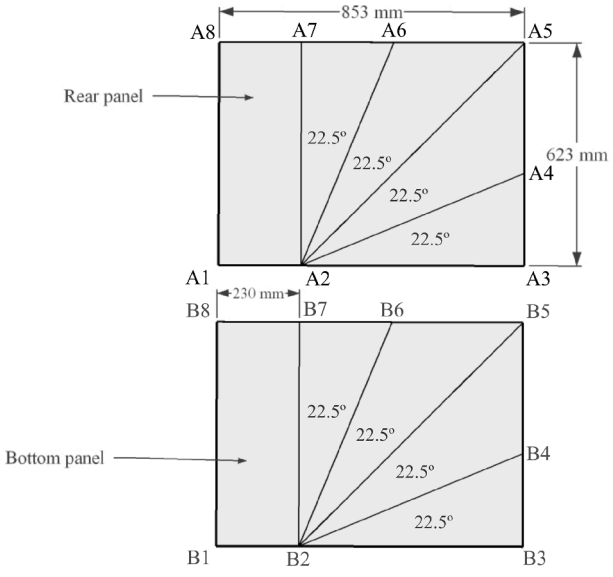

Fig. 1. Representation of cutting lines of the two plates used for building one funnel reflector.

for a range of temperature higher than water boiling point at sea level. They investigated the influence of using the glass cover on the thermal performance. Carrillo-Andrés et al. [23] used a raytracing computational model to study the optical performance and the influence of misalignments on ideal sun tracking. All these works have contributed to a better understanding of the performance of funnel-type solar cookers.

Kumar et al. [28] tested a box solar cooker with a common aluminium black plate placed at the bottom of the cooking chamber and the same box cooker design with a layer of hollow capsules distributed over the aluminium plate. The capsules were filled with a phase change material with a melting temperature of 64 °C. Experiments of testing two box cookers side by side were conducted for investigating the performance of each configuration with load distributed in four pots and also without pots. The reported results indicated that the difference between the stagnation temperatures of the aluminium plate for the two configurations of the cooker tested without pots is small. The use of a phase change material with a low melting point should be had well justified because, at a first view, the use of a phase change material with a melting point over 100 °C would make more sense to be investigated in the context of a cooking process.

Ghosh et al. [29] investigated on the impact of different glazing on the performance of a box solar cooker without load. They found that the use of a cover of single glazed low-e antimony indium oxide coating is promising for domestic usage.

There is an aspect that has not been studied so far, the influence of the load level of the cooking vessel on the cooker performance. In the case of funnel solar cookers, it is quite common to process a small amount of food or water occupying a volume smaller than the full capacity of the cooking vessel (i.e., partial load). From empirical experience of the intensive solar cooking user and co-author of current paper

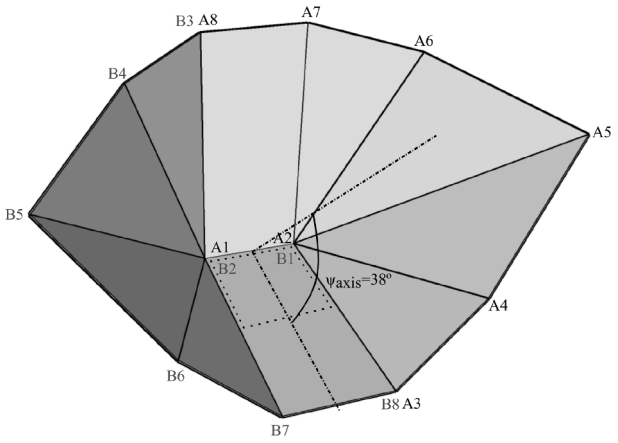

Fig. 2. Assembled funnel reflector.

Table 1
Funnel cooker geometrical data summary.

Central axis elevation angle, ψ_{axis}(°)	38
Funnel collecting area, A_c (cm^2)	4995
Reflective panels total area (cm^2)	10,620
Distance between apexes (mm)	
$\overline{A5B5}$	992
$\overline{B6A4}$	597
Pot diameter (mm)	200
Pot height (mm)	100
Pot total external area (cm^2)	1256
Lid and bottom area (cm^2)	314
Pot side area (cm^2)	628
Transparent enclosure specifications	
Material	Clear glass
Thickness (mm)	5
Height of upper piece of CSR1 (mm)	72
Height of lower piece of CSR1 (mm)	92
Height of upper piece of CSR2 (mm)	71
Height of lower piece of CSR2 (mm)	92
External diameter of upper piece of CSR1 and CSR2 (mm)	275
External diameter of lower piece of CSR1 and CSR2 (mm)	278
Mass of upper piece of CSR1 (g)	1041
Mass of lower piece of CSR1 (g)	1199
Total mass of glass enclosure of CSR1 (g)	2240
Mass of upper piece of CSR2 (g)	1021
Mass of lower piece of CSR2 (g)	1186
Total mass of glass enclosure of CSR2 (g)	2207

Celestino Ruivo, using a partial load influences the cooker thermal performance. This effect has not yet been rigorously investigated. This work aims to fill this lack, through extensive experimental tests of two funnel solar cookers using pots with different load levels. The experimental adopted protocol is based on ASAE S580-1 Standard for a better replicability. Results from experimental tests are correlated into a simple formula of interest to the practical user. A physical interpretation of the results is made, based on how the fill level of the cooking vessel affects its function as a thermal radiation receiver. Finally, a new vessel design that improves performance at partial loads is proposed and tested.

2. Materials and methods

2.1. Description of the funnel solar cooker

The funnel solar cooker uses a multifaceted reflector to concentrate

a)

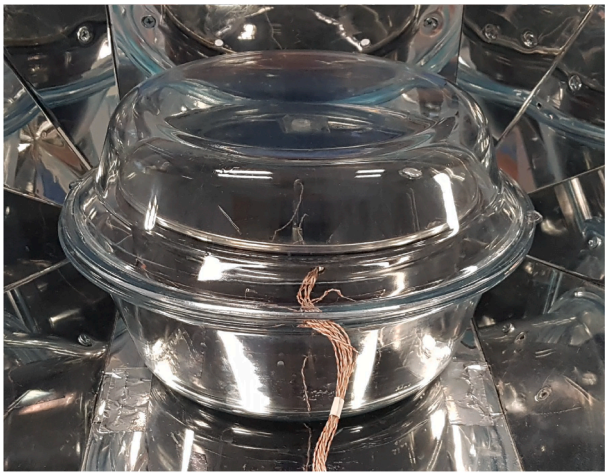

b)

Fig. 4. Cooking set: a) without glass enclosure and b) with glass enclosure.

Fig. 3. Solar cookers CSR1 and CSR2 during a test.

solar radiation on a cooking vessel that is placed inside a transparent enclosure to create a greenhouse effect. The model studied in this work is made from two identical rectangular composite panels, as shown in Fig. 1, with aluminium mirror finish and a solar reflectance of 0.85 [30]. Panels are cut and assembled to form the 3D funnel shape reflector as illustrated in Fig. 2. More details on the construction and assembling of each reflector can be found in Ruivo et al. [20]. Detailed geometrical data can be found in Table 1. A central axis of the funnel reflector can be defined as the intersection of the horizontal and vertical bisector planes. The resulting angle ψ_{axis} shown in Fig. 2 is 38°. The intercept area is the funnel aperture area projected onto a perpendicular plane to direct beam radiation. In this case, the maximum possible intercept area, $A_c = 0.4995\ m^2$, occurs when the sun's rays are parallel to the central axis of the reflector. Two identical funnel reflectors, named CSR1 and CSR2, were constructed and tested side by side. The two complete devices are depicted in Fig. 3.

Regarding the cooking set, the load is contained in a cylindrical, black-enamelled steel cooking pot with a glass lid, 200 mm diameter and 100 mm height, see Fig. 4a). The maximum capacity of the pot is 3 L. The mass of the pot and glass lid are 540 g and 260 g, respectively. Fig. 4b) depicts the pot inside a glass enclosure, which acts as a heat trap. The mass values of the two enclosures are 2250 g and 2207 g, respectively, for CSR1 and CSR2. These massive glass enclosures are made of recycled windows from discarded washing machines. They are 'as new' when properly cleaned. Table 1 lists some other data about these two enclosures. The differences between the mass values and shapes of these two enclosures are negligible. Even though they are not strictly identical, they were used previously in side by side experiments for testing more than one solar cooker [19–22,31]. The results show that the performance of funnel solar cooker tested with these two transparent enclosures can be considered identical. As an example, in Ruivo et al. [20], experiment no. 63, the difference between the measured standardised power of two identical cookers was less than 0.8%. It is important to note that using a massive glass enclosure, 5 mm thick, has a considerable impact on the total mass of the cooking set. Thus, a large amount of the solar energy captured by the funnel reflector is stored in the glass enclosure. As expected, if a greenhouse with negligible mass, such as a thin-walled glass enclosure or a plastic bag, were used instead, the cooker power would be higher. However, these alternatives have disadvantages. There is a risk of breaking a thin glass enclosure when washing it, and plastic bags can only be used a few times and may melt if they come into contact with the cooking pot.

This cooker design does not require the user to be close to the cooker during whole cooking period, because it can successfully cook the food in periods of about 2 h without need of tracking. Moreover, the risk of burning is very small. Cleaning of the funnel reflector is very easy. Simple cleaning operation with water and a soft cloth is enough.

2.2. Parameters of performance

Next, some theoretical background will be presented to support discussion on the influence of the load level on the performance of the cooker. Most of the performance parameters commonly used to rate solar cookers are based on the well-known Hottel-Whillier-Bliss (HWB) [32] formulation:

$$\dot{Q} = A_c F' \eta_0 I - A_r F' U_L (T_w - T_a) \quad (1)$$

where $\dot{Q}$ is the rate of useful heat gain by the water, A_c is the collecting area of the funnel reflector, η_0 is the optical efficiency, defined as the fraction of incident solar radiation on the collecting area that is absorbed at the pot surfaces, I is the total solar irradiance on the collecting area, and A_r is the receiver area, i.e., the surfaces of the pot that absorb solar radiation. The parameter U_L represents the heat loss factor, T_w the water temperature, T_a the ambient temperature and F' the heat exchange efficiency factor. The parameter F' represents the ratio of actual useful energy gain to the useful gain that would result if the receiver absorbing surface had been at the water temperature [32]. F'multiplies both the heat loss factor U_L and the optical efficiency η_o. The efficiency of the cooker can be defined as the ratio of useful heat gain to the solar energy intercepted by the funnel reflector, Eq. (2):

$$\eta = \frac{\dot{Q}}{A_c I} \quad (2)$$

Combining Eqs. (1) and (2), a common form of HBW formulation is obtained:

$$\eta = \frac{\dot{Q}}{A_c I} = F' \eta_0 - \left(\frac{F' U_L}{C_g}\right) \frac{(T_w - T_a)}{I} \quad (3)$$

where $C_g = A_c/A_r$ is the cooker geometric concentration ratio. In the case of this cooker $C_g = 3.97$. More details can be found in the work of Carrillo-Andrés et al. [23].

The pair of parameters $F'\eta_0$ and $\frac{F' U_L}{C_g}$ is usually determined experimental. In a typical test, a certain load inside a pot, water or other suitable fluid, is placed in the solar cooker and heats up in the sun. Solar irradiance, ambient temperature and water temperature are recorded during the experiment. Useful heat gain rate is calculated from the rate of increase in water temperature by:

$$\dot{Q}_i = m_w c_w \frac{dT_w}{dt} \quad (4)$$

where m_w and c_w are the mass and the specific heat of water, respectively. The experimental data is used to plot $\frac{\dot{Q}}{A_c I}$ vs $\frac{(T_w - T_a)}{I}$, and a linear fit gives the parameters $F'\eta_0$ and $\frac{F' U_L}{C_g}$. This linear formulation has some limitations [33], but it is the most frequently used to date and is the basis for some of the most widely used methods for evaluating the performance of solar cookers. For example, the recently proposed opto-thermal ratio performance parameter (*COR*) is simply related by [23,25,34]:

$$COR = \frac{\eta_0 C_g}{U_L} \quad (5)$$

The widely accepted ASAE S580.1 standard [26,27] protocol for testing and reporting solar cooker thermal performance also proposes a linear formulation. More details can be found in Section 2.6.

2.3. Influence of partial load on the cooker performance

In the case of funnel solar cookers, it is quite common to cook with a partial load, i.e., to process a small amount of food or water occupying a volume smaller than the full capacity of the cooking vessel. In fact, ASAE S580.1 Standard indicates a specific load ratio to be used in the tests, defined as the ratio between the water load and the intercept area of the cooker: "*cookers shall have 7,000 g potable water per square meter intercept area distributed evenly between the cooking vessels supplied with the cooker. If no cooking vessels are provided, inexpensive aluminium cooking vessels painted black shall be used*". In this work, this parameter is denoted as "*load-to-area ratio*", *LAR*:

$$LAR = \frac{m_w}{A_c} \quad (6)$$

Funk [26] mentioned that water was chosen as working fluid in ASAE S580.1 because it resembles food in density and specific heat. He declared that "*thermal performance is sensitive to loading rate*", but he did not offer more details on this aspect.

In an early work by Mullick et al. [35], it was observed, for a box type cooker, that cooker performance increased with increase of water load. This result was attributed to an improvement in the ratio between the capacity of the water load and the added capacity of water, vessels, and a certain portion of the interior of the cooker. Mullick et al. [35] also

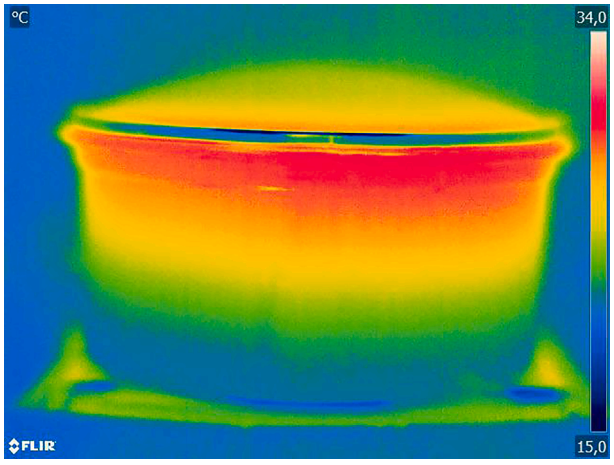

Fig. 5. Thermal image of a pot with partial load during a heating test inside the funnel reflector.

Table 2
Instruments used to measure the solar irradiance, air speed and temperature.

Variable	Instrument	Operation range	Technical specifications
Global solar irradiance (W m^{-2})	LP02 pyranometer (Hukseflux)	0 to 2000	Calibration uncertainty < 1.8%
Global solar irradiance (W m^{-2})	LP02 pyranometer (Hukseflux)	0 to 2000	Calibration uncertainty < 1.8%
Global solar irradiance (W m^{-2})	CM 21 pyranometer (Kipp & Zonen)	0 to 4000	Accuracy expected maximum errors: 2%
Diffuse solar irradiance (W m^{-2})	SPN1 pyranometer (Delta-T Devices ltd)	0 to 2000	Overall accuracy: ±8% ±10 W m^{-2}
Air speed (m s^{-1})	3 cup anemometer S-WSB-M003 (Hobo Onset)	0 to 76	Accuracy: ±4% of reading whichever is greater. Resolution: 0.5 m s^{-1}
Ambient temperature (°C)	Thermistor S-TMB-M002 (Hobo Onset)	−40 to 75	Accuracy < ±0.2 °C from 0 to 50 °C
Temperature of water (°C)	Thermocouple type T (TC Ltd.)	−75 to 250	Tolerance value: ±1.0 °C

investigated the effect of number of vessels, keeping the total water load constant. They found that performance increased with the number of vessels, which was attributed to an improvement in the heat-exchange efficiency factor F', which indicates the effectiveness of the heat transfer from the plate or the vessel top to the contained load. As the latter results are obtained with a constant *LAR*, it suggests that the geometric configuration of the space occupied by the load may influence the thermal performance of the cooker. In the case of a funnel solar cooker, solar radiation hits mainly on the lid and side of the pot [23]. Consequently, the absorbing surfaces increase their temperature, driving the heat to the water load. A pot full of water is much more efficient as a receiver because the temperature of irradiated surfaces in contact with water tends to be closer to that of water, as the convection heat transfer between pot walls and water is very effective. Heat transfer to the water is very effective when solar radiation impinges the outside face of the pot side below the water line, or when radiation passes through a glass lid and the water itself, and then is absorbed at the inside face of the pot side, below the water line, or at the bottom of the pot. On the opposite side, when the solar radiation impinges the side of the pot at its outside face above the water line, the heat transfer is not so effective. The metal of the pot wall acts as an extended surface like a fin, but its temperature will inevitably rises above the water temperature, causing more heat losses to the external environment. This effect is depicted in Fig. 5, that shows an infrared image of the pot made on December 17, 2021, with 1.5 kg partial water load, glass lid. The image was made 9 min after starting the ~~a~~ heating test of load using cooking vessel, without enclosure. It can be noticed how the side wall of the pot has a much higher temperature in the part that is above the water line.

The increase in temperature of the absorbing surface over that of water is very noticeable in the case of using an opaque lid. In the work of Ruivo et al. [20], the temperature of a black metal lid was measured, being much higher than that of the water load and easily reaching temperature differences of around 100 °C. The associated increase in heat losses to the environment can be significant. In fact, the use of a glass lid increased standardised cooker power [27] by 46% compared to the use of a metal lid [20].

From the point of view of the HWB model, a reduced water load leads to a decrease of the heat exchange factor F', but also changes in parameter U_L may be possible, since natural convection and long wave radiation exchange are dependent on the surface temperature. In view of the above, it follows that predicting the influence of the load level on the cooker performance is a complex task, since very detailed optical and thermal models are necessary. An alternative approach is experimentation, then correlating the results with some significant parameter. Since the filling level of the vessel is important, it is convenient to introduce a new parameter here named *"volumetric load fraction"*. It is defined as ~~is~~ the ratio of the volume occupied by the water load (V_w) to the total volume of the cooking vessel (V_{pot}):

$$VLF = \frac{V_w}{V_{pot}} \tag{7}$$

For a given intercept area and pot volume, water load is related with *LAR* and *VLF*, but they focus on different concepts.

2.4. Experimental set-up

Two identical funnel cooker reflectors, CSR1 and CSR2, were tested side by side as shown in Fig. 3. The experimental set-up was installed outdoors, on the roof of the School of Industrial Engineering of the University of Malaga, Spain, at a latitude of 36.9°N. Tests were conducted from November 2019 to February 2020 and in January and February 2021. Only azimuthal sun tracking was applied, i.e., each prototype was tested without tilting adjustment. Five *T*-type thermocouples having and uncertainty of ± 1 °C were positioned 10 mm from the bottom of the pot to measure the temperature of the water. One sensor is in the centre of the pot and the positions of the other four sensors form a square whose vertices are all approximately 10 mm from the pot wall. The average temperature value, $\overline{T}_w$, provides a more robust measure of the water temperature than using the value of single sensor. Global solar irradiance was measured by two Hukseflux LP02 pyranometers near the cookers. One was placed horizontally, and the other was placed on a tilted plane at an angle of 40° to the horizontal plane. Global normal solar irradiance I_n and direct normal solar irradiance I_{bn} were computed from measurements of the two pyranometers measurements, using the Liu Jordan isotropic sky model [32]. The albedo was assumed to be 0.2 and the diffuse fraction of global radiation was taken from data measured in a nearby meteorological station. A Campbell Scientific CR1000 data logger recorded both global solar irradiance and temperature every minute. Wind speed and ambient temperature were measured by a dedicated Onset weather station located near the cookers. Measurement ranges and technical specifications of the used instruments are summarized in Table 2.

2.5. Test cases

The *LAR* value recommended by ASAE S580.1 Standard is 7 kg m^{-2}.

Table 3
Test cases considered.

Cases with glass enclosure	G1	G2	G3	G4
Cases without glass enclosure	N1	N2	N3	N4
Water load, m_w (kg)	0.5	1	1.5	2
Load to area ratio, *LAR* (kg m^{-2})	1	2	3	4
Volumetric load fraction, *VLF* (-)	0.167	0.333	0.500	0.667

This value does not correspond to the most common solar cooking operations in real daily practice. Moreover, the dimensions of the pot and the amount of food load adopted in practice with the funnel cooker tested are not compatible with the standard load ratio. Thus, different amounts smaller than the value recommended by the ASAE S580.1 Standard have been tested. Each test with different amount of water corresponds to a different load to area ratio (*LAR*) and also to a different level of load inside the cooking vessel when the same pot is used. The *LAR* values tested in this work are 4, 3, 2 and 1 kg m^{-2}, corresponding to 2.0, 1.5, 1.0 and 0.5 kg water load, as indicated in Table 3. The lower ratios correspond, for example, to the amount of water needed for preparing tea or coffee for two or three people. Each water load is also related to the portion of absorbing surfaces below or above the waterline, see Fig. 6.

A total of 46 individual tests have been carried out. Data for each individual test can be found in Tables A1 and A7 included in Appendix A. Part of the tests were carried out without glass enclosure to determine if the presence of this element influences the impact of partial loads on performance. As shown in Table 3, there are a total of eight test cases. Cases with glass enclosure are indicated with the letter G, whereas cases without glass enclosure are indicated with the letter N.

2.6. Data processing

The standardised power of cookers CSR1 and CSR2 for the two configurations of cooking set and for different mass values of the water load was evaluated by following mainly the protocol of ASAE S580.1 Standard [27]. Water was heated from ambient temperature until a point close to the boiling point, typically around 95 °C. When starting each experiment, the pot, the lid, and the glass enclosure were at a temperature close to the ambient temperature because they had not yet been exposed to the sun. The measured values of all variables are clustered in time intervals. For each time interval Δt_i, the water temperature increases by $\Delta T_{w,i}$ and the cooker power $\dot{Q}_i$ is computed using:

$$\dot{Q}_i = \frac{m_w c_w \Delta T_{w,i}}{\Delta t_i} \tag{8}$$

where m_w and c_w are the mass and the specific heat of water, respectively. The mass of water inside the pot is assumed to be constant because, as boiling point is not achieved, the mass of water changing to vapour is negligible during a test.

As recommendation of ASAE S580.1 Standard [27], the cooker power at each time interval is corrected to a reference value for a global normal solar irradiance of 700 W m^{-2}, using:

$$\dot{Q}_{S,i} = \dot{Q}_i \frac{700}{I_{n,i}} \tag{9}$$

The standardised cooker power of all valid observation points is then plotted against the difference between the water temperature and the ambient temperature and the following linear regression linear, relating the standardised cooker power $\dot{Q}_S$ and the temperature difference, is determined:

$$\dot{Q}_S = \dot{Q}_{S,0} + a\Delta T_{w,a} \tag{10}$$

The ASAE S580.1 Standard promotes the use of a single measure of performance $\dot{Q}_{S,50}$ that is the standardised cooker power for $\Delta T_{w,a} = 50$ °C and a standard value solar irradiance $I = 700$ W m^{-2}, predicted by the linear regression of Eq. (10). This value is deemed to be representative of the cooker power throughout the process of heating water from ambient temperature to the boiling point. The global normal solar irradiance was adopted because it leads to a fairer comparison between cooker designs, as many solar cookers can collect diffuse solar radiation, at least in some extension. Besides it is a recommendation of ASAE

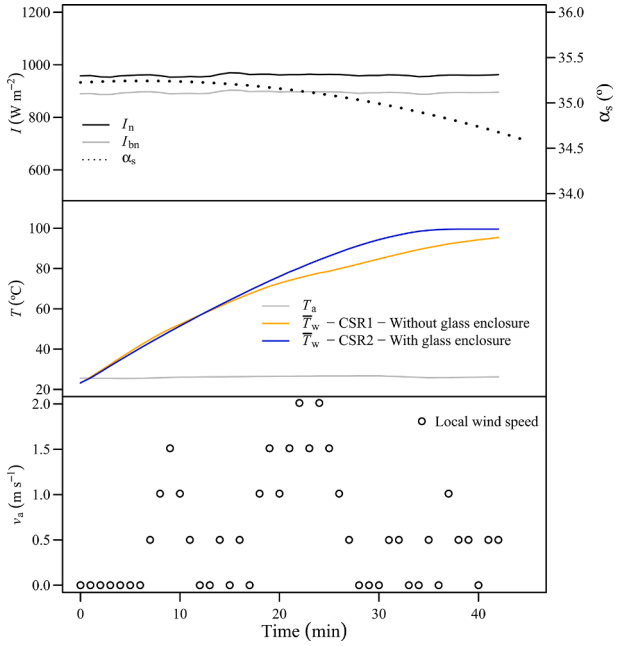

Fig. 7. Time series of several variables during test of cookers CSR1 and CSR2 in experiment 109B by using 0.5 kg of water.

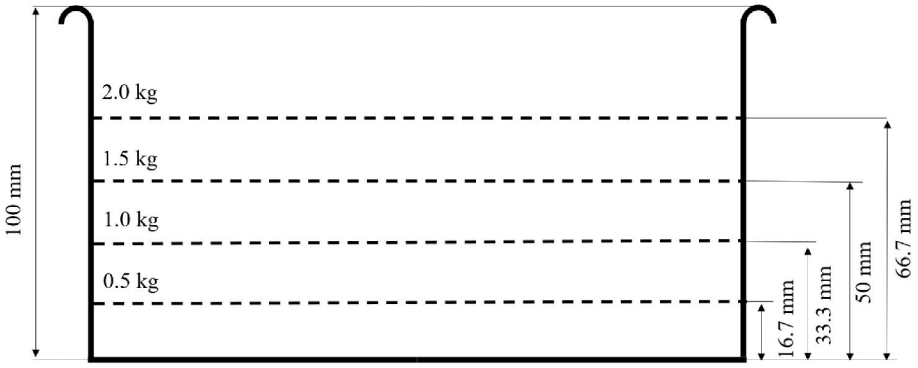

Fig. 6. Water line height h_w for different load levels.

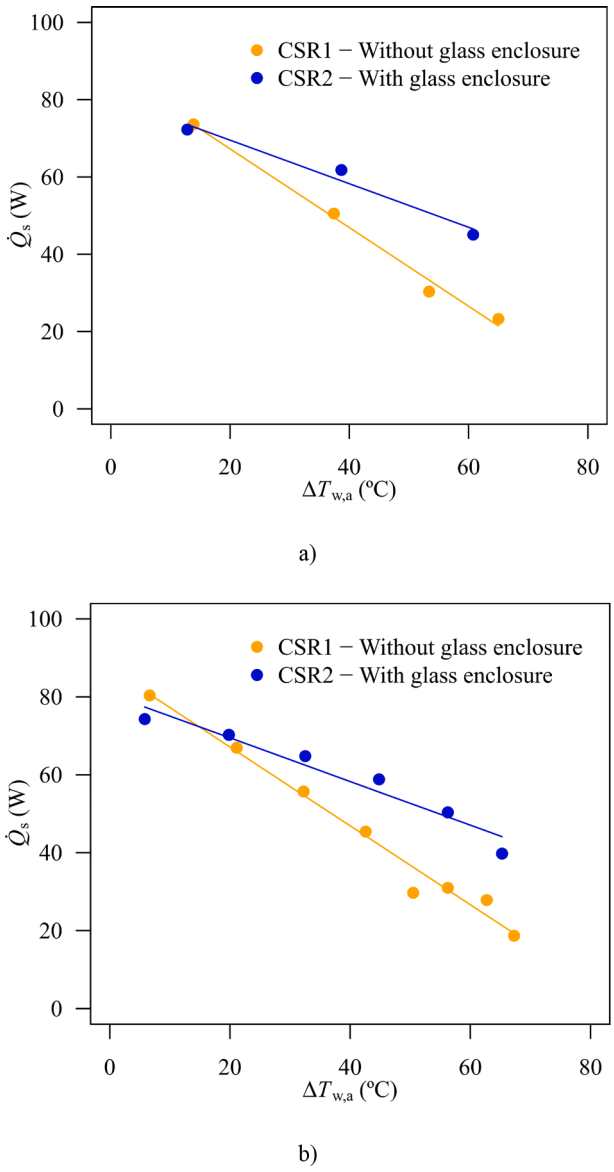

Fig. 8. Plots of standardised power of cookers CSR1 and CSR2 for the experiment 109B with clustering time interval of a) 10 min and b) 5 min.

Table 4
Summary of regression analysis of tests with 0.5 kg water load, for clustering time intervals of 10, 5 and 3 min.

Cooking set	with glass enclosure			without glass enclosure		
Δt_i(min)	10	5	3	10	5	3
n_p	21	42	71	25	44	78
$\dot{Q}_{S,0}$(W)	74.1	77.8	78.1	68.4	77.9	76.7
a (W °C^{-1})	−0.498	−0.567	−0.578	−0.718	−0.871	−0.859
R^2	0.855	0.898	0.896	0.849	0.930	0.919
$\dot{Q}_{S,50}$(W)	49.2	49.5	49.2	32.5	34.3	33.8
$\dot{Q}_{S,50,CI95\%}$(W)	(47.1, 51.3)	(48.3, 50.7)	(48.3, 50.1)	(29.7, 35.4)	(32.9, 35.8)	(32.6, 35.0)
$\dot{Q}_{S,50,PI95\%}$(W)	(40.4, 58.1)	(42.0, 56.9)	(41.6, 56.8)	(18.3, 46.7)	(24.8, 43.9)	(23.4, 44.2)

S580.1 Standard. If normal direct solar irradiance values were used in Eq. (9), considering 90% of 700 W m^{-2} as the corresponding standard direct solar irradiance value, the obtained standardised power values, in the case of present study, would not change strongly because, according to the data published in Tables A1 to A7, the average fraction of direct solar irradiance is 0.902, being the maximum and the minimum fraction values 0.942 and 0.821. As water load changes, it is convenient to introduce a standardised power per unit of mass load, to provide a better description of the cooker performance at partial loads:

$$\dot{q}_{S,m,50} = \frac{\dot{Q}_{S,50}}{m_w} \tag{11}$$

where m_w is the mass of water.

In this work, the 10-minute clustering time interval specified in the ASAE S580.1 Standard was found to be too large to adequately sample short duration tests. As an example, Fig. 7 shows the time series for some relevant variables measured during the experiment 109B, conducted on 29th January 2021, using funnel reflectors, CSR1 without the glass enclosure and CSR2 with the glass enclosure, with just 0.5 kg of water. This experiment started at 11:54 am (solar time) and took just about 40 min to finish. Once the data is processed, Fig. 8a) shows the results of standardised power values for the experiment 109B. Only three valid points were obtained to describe the whole heating process when using the Standard clustering time interval of 10 min. This low sampling frequency may cause a loss of information when deriving the linear regression used for estimation of the standardised power. Using a reduced interval of 5 min seems to be more adequate, Fig. 8b). However, to justify the decision on which time interval to adopt, the entire set of experiments with 0.5 kg of water load was analysed in time intervals of 3, 5 and 10 min.

Table 4 summarises the data and results of the calculations of some parameters, operating with 0.5 kg of water, for time intervals of 10, 5 and 3 min. It was found that some regression parameters have differences up to 18% when comparing the results obtained with time intervals of 10 min and 5 min. The largest difference, 18%, is observed on the slope (a) of the linear regression for the cooking set configuration not using the glass enclosure. For the same configuration, the difference on $\dot{Q}_{S,0}$ and $\dot{Q}_{S,50}$ are 12% and 5%, respectively. These findings suggest that information was lost when using a time interval of 10 min. When comparing the results obtained with time intervals of 5 and 3 min, those differences are practically negligible, so it is concluded that a time interval of 5 min is adequate to sample short-duration tests.

On the other hand, to validate the adequacy of a 5 min clustering time for slow tests, the same analysis is applied to the set of experiments using 2 kg water load, i.e., for a *LAR* of 4 kg m^{-2}. Table 5 lists the calculated parameters. It can be observed that regression parameters are practically the same for time intervals of 10 and 5 min. Therefore, a time interval of 5 min is an adequate clustering time interval to process the entire range of slow and fast tests conducted in this work. Finally, confidence and prediction intervals were computed for the standardised cooker power. A confidence interval reflects the uncertainty around the mean prediction values, while a prediction interval reflects the uncertainty around a single value [36]. The use of confidence and prediction intervals is considered an improvement on the ASAE S580.1 Standard data processing protocol. The R language [37] was used for the data

Table 5
Summary of regression analysis of tests with 2 kg water load, for different clustering time interval of 10 and 3 min.

Cooking set	with glass enclosure		without glass enclosure	
Δt_i(min)	10	5	10	5
n_p	68	133	30	56
$\dot{Q}_{S,0}$(W)	105.2	105.7	99.2	99.6
a (W °C^{-1})	−0.617	−0.621	−0.874	−0.874
R^2	0.800	0.806	0.82	0.809
$\dot{Q}_{S,50}$(W)	74.3	74.7	55.5	55.7
$\dot{Q}_{S,50,CI95\%}$(W)	(72.9, 75.7)	(73.7, 75.6)	(52.8, 58.2)	(53.8, 57.6)
$\dot{Q}_{S,50,PI95\%}$(W)	(63.1, 85.5)	(64.1, 85.2)	(40.7, 70.2)	(41.8, 69.7)

Table 6
Summary of regression analysis of tests with different load ratios by using cooking sets without glass enclosure.

Configuration	N1	N2	N3	N4
m_w (kg)	0.5	1.0	1.5	2.0
LAR (kg·m^{-2})	1	2	3	4
VLF (-)	0.167	0.333	0.500	0.667
n_t/ n_{t1} /n_{t2}	5 / 2 / 3	2 / 1 / 1	3 / 3 / 0	3 / 2 / 1
n_p	44	27	40	56
$\dot{Q}_{S,0}$(W)	77.9	88.6	97.8	99.6
a (W °C^{-1})	−0.871	−0.895	−1.01	−0.878
R^2	0.93	0.97	0.931	0.809
$\dot{Q}_{S,50}$(W)	34.3	43.9	47.3	55.7
$\dot{Q}_{S,50,CI95\%}$(W)	(32.9, 35.8)	(42.7, 45.1)	(45.7, 49.0)	(53.8, 57.6)
$\dot{Q}_{S,50,PI95\%}$(W)	(24.8, 43.9)	(37.8, 50.1)	(38.3, 56.4)	(41.8, 69.7)
$\dot{q}_{S,m,50}$(W kg^{-1})	68.6	43.9	31.5	27.9

Table 7
Summary of regression analysis of tests with different load ratios by using cooking sets with glass enclosure.

Configuration	G1	G2	G3	G4
m_w (kg)	0.5	1.0	1.5	2.0
LAR (kg m^{-2})	1	2	3	4
VLF (-)	0.167	0.333	0.500	0.667
n_t/ n_{t1} /n_{t2}	7 /6 / 1	5 /3 / 2	5 /2 / 3	10 / 3 / 7
n_p	42	62	65	133
$\dot{Q}_{S,0}$(W)	77.8	88.1	97.0	105.7
a (W °C^{-1})	−0.567	−0.706	−0.681	−0.621
R^2	0.898	0.916	0.735	0.806
$\dot{Q}_{S,50}$(W)	49.5	52.7	62.9	74.7
$\dot{Q}_{S,50,CI95\%}$(W)	(48.3, 50.7)	(51.5, 54.0)	(60.8, 65.1)	(73.7, 75.6)
$\dot{Q}_{S,50,PI95\%}$(W)	(42.0, 56.9)	(43.3, 62.2)	(47.6, 78.3)	(64.1, 85.2)
$\dot{q}_{S,m,50}$(W kg^{-1})	99.0	52.7	41.9	37.4

processing, linear model fitting, and graph production.

3. Results and discussion

Table 6 summarizes results for the four tested configurations N1 to N4, without glass enclosure. The total number of tests carried out is denoted by n_t, being n_{t1} and n_{t2} the number of tests perfomed with devices CSR1 and CSR2, respectively. Similarly, Table 7 shows results for the four tested configurations, G1 to G4, with glass enclosure.

Figs. 9 to 12 show the regression analysis for *LAR* values of 1, 2, 3, and 4 kg m^{-2}, respectively. A visual inspection suggests there may be a non-negligible dependency of power of the cooker on the sun elevation angle. Tests conducted with a sun elevation angle close to the central axis of the cooker (~38°) tends to deliver more power as can be seen, for example, in the results of the experiments 60A with CSR1 and 60A with CSR2, compared to the other tests plotted in the same Fig. 11. Future works should investigate, in more detail, the influence of the sun elevation angle on the cooker performance. However, in this work, all tests were conducted within a limited range of average values of sun elevation angle, i.e., in the range of 28 to 41°. Thus, the impact of the sun elevation angle on the performance of the cooker, for the experiments carried out in present work, is also limited. Moreover, the dispersion of data seems to be acceptable because the R^2 values comply with the ASAE S580.1 Standard, being relatively high in all tests, except for the configuration G3. In this set of tests, shown in Fig. 6 in blue colour, the R^2 value is at the limit of the Standard.

The results summarized in Table 8 show clearly that lower load ratios lead to lower cooker power values $\dot{Q}_{S,50}$, and $\dot{Q}_{S,0}$. This phenomenon has already been verified by the authors in other recent published works [17,19], as it can be seen also in Table 9. The relationship between mass load and the $\dot{Q}_{S,50}$ and $\dot{Q}_{S,0}$ parameters was not investigated in these two previous works [17,19]. According to the plots depicted in Fig. 13, a linear trend is observed. The dotted lines shown in Fig. 13 represent the extrapolation of the linear correlations. This linear behaviour is in accordance with what was stated previously in Section 2.3.

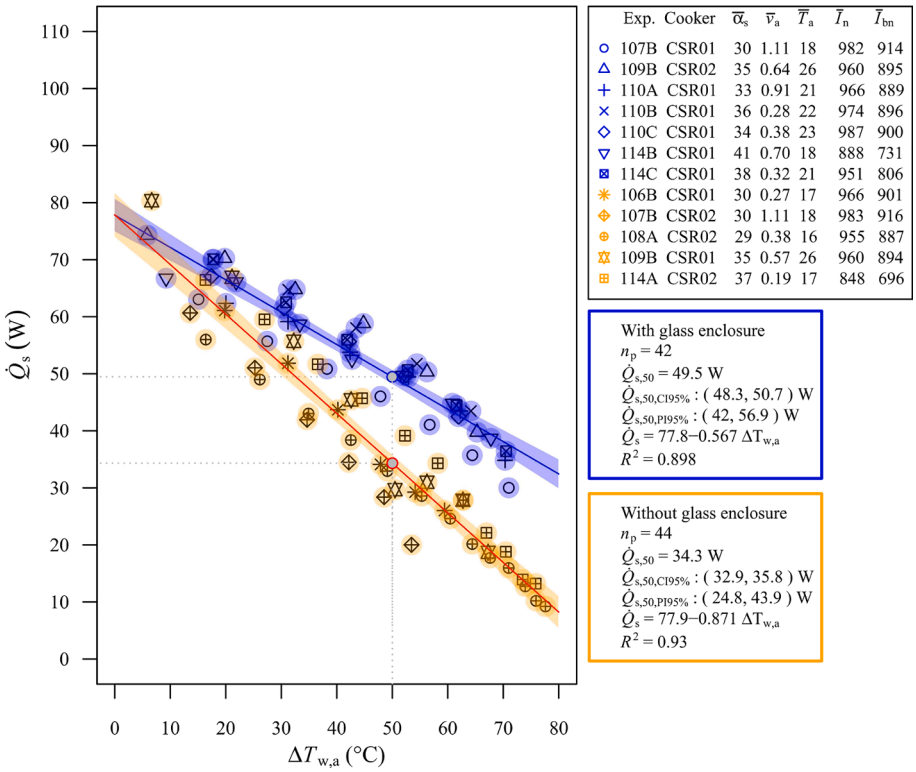

Fig. 9. Regression analysis for G1 and N1 tests adopting 0.5 kg of water, *LAR* = 1 kg m^{-2} and *VLF* = 0.167.

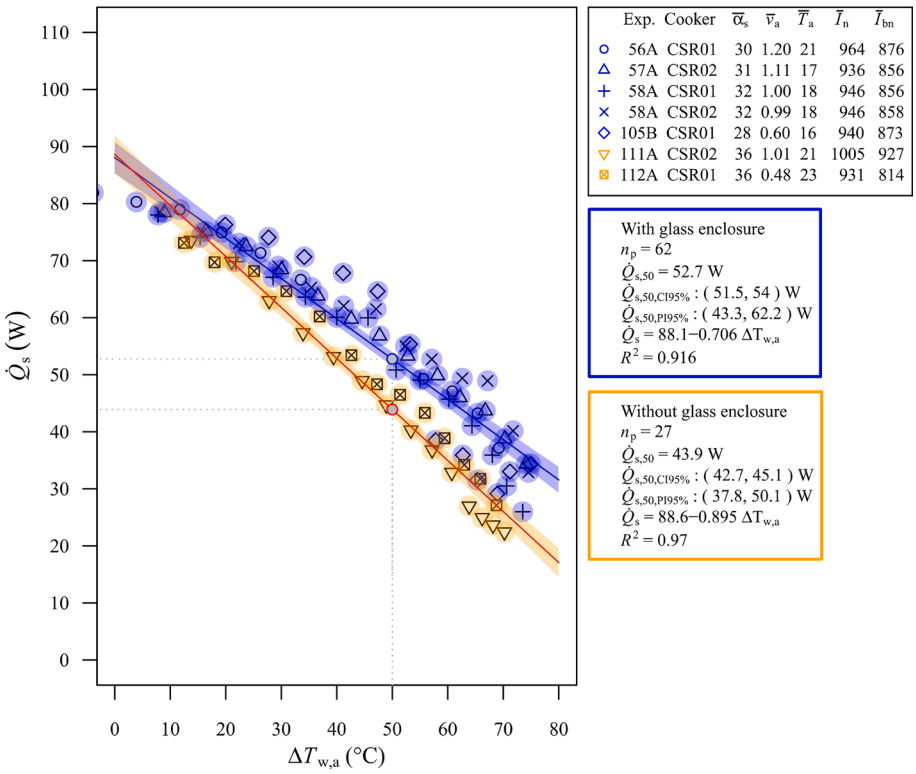

Fig. 10. Regression analysis for G2 and N2 tests adopting 1.0 kg of water, $LAR = 2$ kg m^{-2} and $VLF = 0.333$.

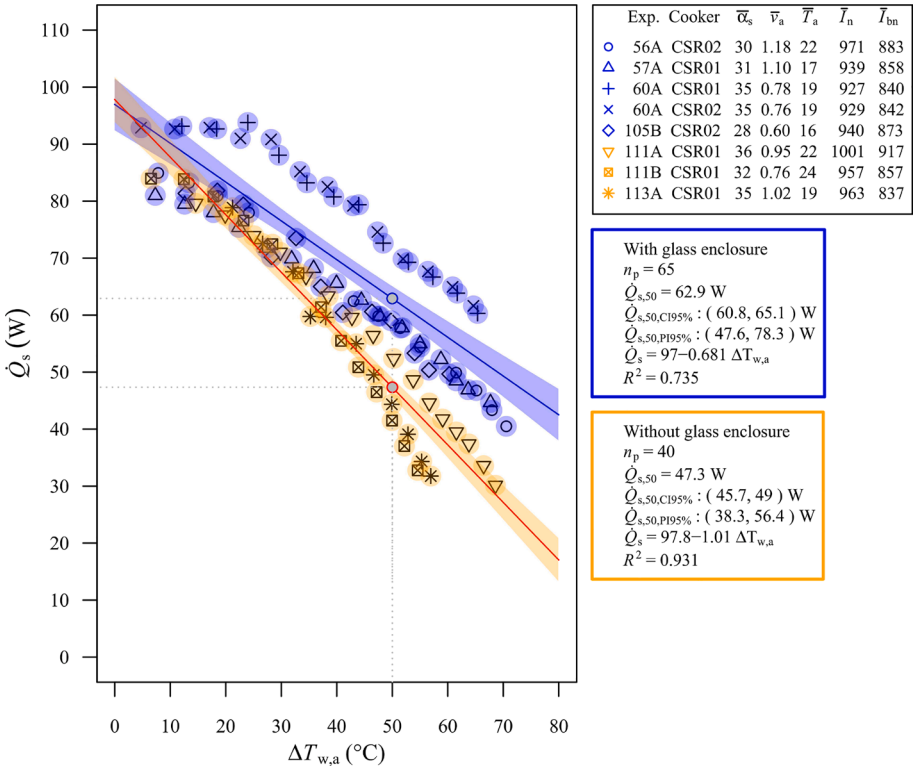

Fig. 11. Regression analysis for G3 and N3 tests adopting 1.5 kg of water, $LAR = 3$ kg m^{-2} and $VLF = 0.500$.

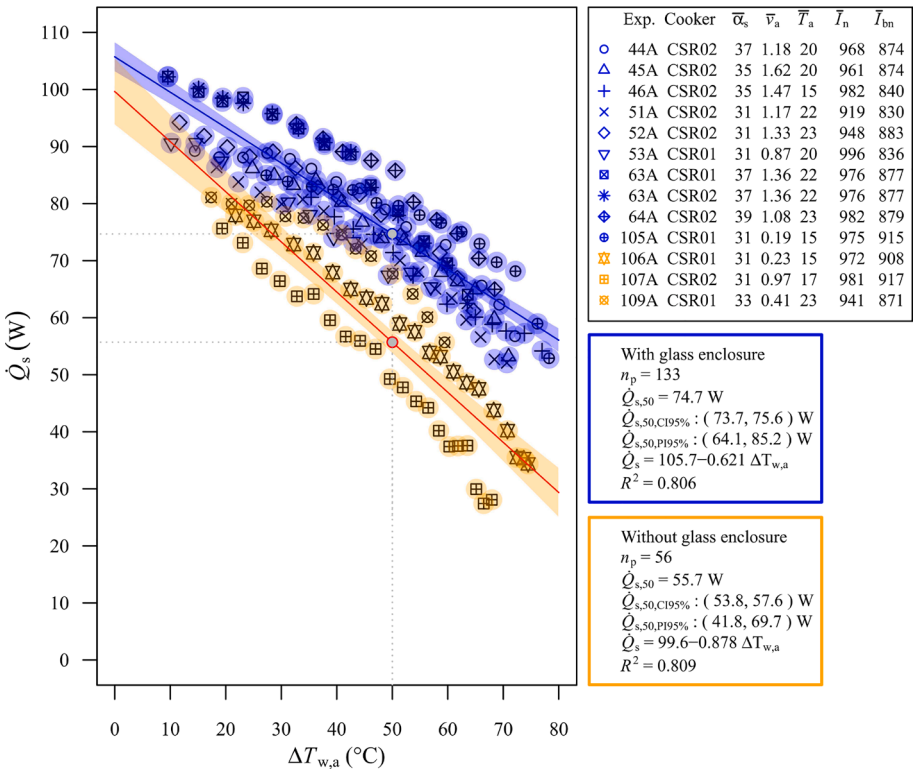

Fig. 12. Regression analysis for G4 and N4 tests adopting 2.0 kg of water, *LAR* = 4 kg m^{-2} and *VLF* = 0.6667.

Table 8
Summary of cooker power for the eight tested configurations.

Mass load (kg)	0.5	1.0	1.5	2.0
LAR (kg m^{-2})	1	2	3	4
VLF (-)	0.167	0.333	0.500	0.667
Experiments without glass enclosure				
Configuration	N1	N2	N3	N4
$\dot{Q}_{S,0}$ (W)	77.9	88.6	97.8	99.6
$\dot{Q}_{S,50}$ (W)	34.3	43.9	47.3	55.7
Experiments with glass enclosure				
Configuration	G1	G2	G3	G4
$\dot{Q}_{S,0}$ (W)	77.8	88.1	97.0	105.7
$\dot{Q}_{S,50}$ (W)	49.5	52.7	62.9	74.7
Increment of $\dot{Q}_{S,50}$ due to the use of glass enclosure (%)	44.3	20.0	32.9	34.1

Table 9
Performance results summary of some solar cookers tested with different water loads.

Solar cooker model	A_c	$\dot{Q}_{S,0}$	$\dot{Q}_{S,50}$	m_w	*VLF*
	(m^2)	(W)	(W)	(kg)	(-)
Copenhagen [19] – *NFN Configuration*	0.197 – 0.238	38.5	11.9	0.5	0.167
Copenhagen [19] – *NFN Configuration*	0.197 – 0.238	43.2	17.5	1.0	0.333
Copenhagen [19] – *NFN Configuration*	0.197 – 0.238	47.1	18.0	1.5	0.500
Haines 2 [17] – *Red Configuration*	0.452	105.0	67.2	2.0	0.444
Haines 2 [17] – *Red Configuration*	0.452	126.9	87.5	3.5	0.778
Haines 2 [17] – *Blue Configuration*	0.475	112.3	65.1	2.0	0.444
Haines 2 [17] – *Blue Configuration*	0.475	140.6	87.7	3.5	0.778

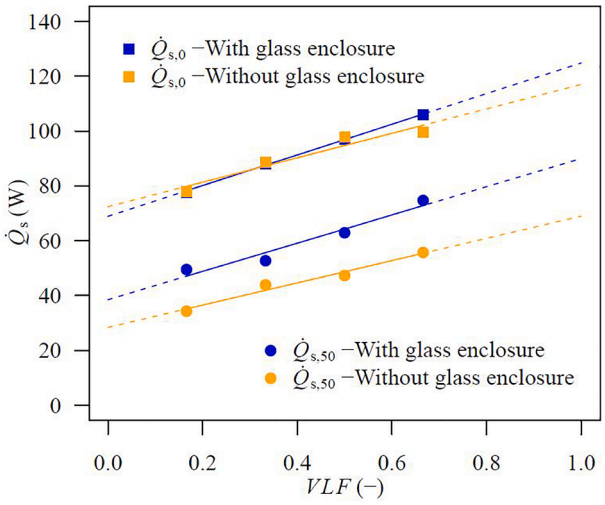

Fig. 13. Influence of water load on the $\dot{Q}_{S,50}$ and $\dot{Q}_{S,0}$ parameters.

Table 10
Proposed formulas for predicting $\dot{Q}_{S,0}$ and $\dot{Q}_{S,50}$ as a function of *VLF*.

Cooking set	without glass enclosure	with glass enclosure
Formula for $\dot{Q}_{S,0}$	$\dot{Q}_{S,0}$ = 72.4 + 44.6*VLF*	$\dot{Q}_{S,0}$ = 69.0 + 55.6*VLF*
Formula for $\dot{Q}_{S,50}$	$\dot{Q}_{S,50}$ = 28.4 + 40.6*VLF*	$\dot{Q}_{S,50}$ = 38.5 + 51.5*VLF*

The parameter $\dot{Q}_{S,0}$ corresponds to the power when difference between water load temperature and ambient is null, $\Delta T_{w,a} = 0$ °C. Thus, the power $\dot{Q}_{S,0}$ is mainly related to the optical efficiency, but heat losses have also influence on it, as explained below. When $\Delta T_{w,a} = 0$ °C, thermal losses from the cooking set to the environment are reduced, but

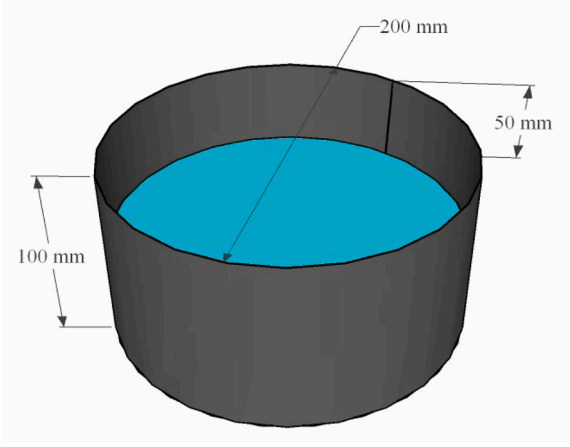

a)

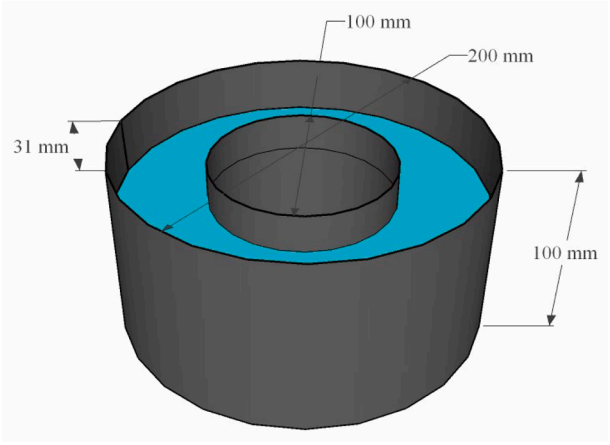

b)

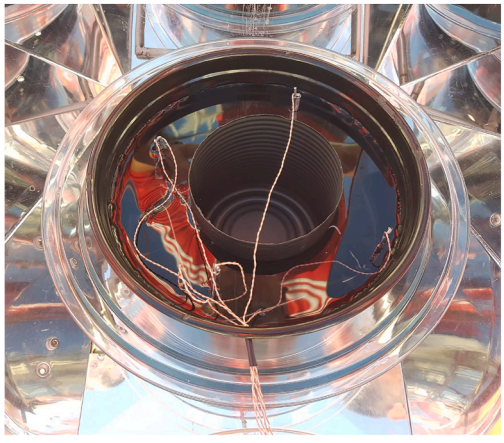

c)

Fig. 14. Cooking vessel: a) standard pot, b) improved vessel, c) photo of improved vessel.

they are not zero. There are pot surfaces that receive solar radiation and achieve higher temperature than that of the water. Those parts of the side wall of the pot that are above the waterline tend to reach a much higher temperature than those below the waterline, see Fig. 5. The same applies to an opaque lid. These high surface temperatures increase the rate of heat losses to the environment. Therefore, an under-filled pot is a low-efficiency radiation receiver. This explains the strong influence of load on $\dot{Q}_{S,0}$. In the case of $\dot{Q}_{S,50}$, the relationship with load is similar to that of $\dot{Q}_{S,0}$. This is expected, as load affects the heat exchange parameter F', that multiplies both the optical and thermal losses terms in the linear model, as was explained in Section 2.3.

Since the influence of partial load on the cooker performance is very strong, it is of interest to the practical user to have a simple linear formula, see Table 10, to estimate the change in performance parameters when using partial loads.

Hence, as a general conclusion, it is desirable to work with a cooking vessel as full as possible, to get the most power from the cooker. However, the standardised power $\dot{q}_{m,S,50}$ per mass load unit (W kg^{-1}) is still higher at partial loads, see Tables 6 and 7. So, a lower load will achieve boiling temperature faster.

Secondarily, it is interesting to analyse the impact of the glass cover on cooker performance. Results show that differences in $\dot{Q}_{S,0}$ between cases with or without glass enclosure are small and within the uncertainty bands. So, results are not conclusive, see Fig. 13. It seems that, in cases without glass enclosure, the higher thermal losses are compensated with an increment of optical efficiency (no glass transmission losses), and a lower thermal inertia (no massive glass to be heated). On the contrary, in the case of $\dot{Q}_{S,50}$ there is a significant influence of the glass cover. The increment in standardised power $\dot{Q}_{S,50}$ is around 30 to 40%. Results for 1 kg water load are a bit off the mark. A possible reason is that, for that water load value, tests performed without glass enclosure were conducted with a noticeably higher sun elevation angle than those tests with glass enclosure, see Fig. 1. For the practical user, a rule of thumb can be stated: when the volumetric load fraction drops by 25%, the standardised power will drop by about 15% of the original value. This rule applies to both operations with and without glass enclosure.

4. Improved cooking vessel design for partial loads

A device is proposed to increase the volumetric load fraction (*VLF*) when using partial loads. This device is a hollow cylinder made of black metal, like a steel can, weighing 57 g. It was inserted in the centre of the cooking vessel, as depicted in Fig. 14. In the scope of the conducted experiments, it was attached to the bottom of the pot using high temperature resistant aluminium foil tape. All added elements were black painted. This is only a concept prototype. It is possible to develop a more practical design of this concept, but it is out of the scope of this work. Side-by-side tests using 1.5 kg water load, and adopting a glass enclosure, were conducted to evaluate the cooker performance with a standard vessel and with an improved vessel. The obtained results are depicted in Fig. 15. The use of this cylindrical device causes an increase of *VLF* from 0.50 to 0.64. Standardized power of the cooker with standard vessel was $\dot{Q}_{S,50} = 54.2$ W. This result agrees with the result of other tests made using the same load, with similar sun elevation angle $\alpha_s \approx 30^{\circ}$ (experiments 56A with CSR2, 57A with CSR1 and 105B with CSR2, see Table A3). The standardized power $\dot{Q}_{S,50}$ increases to 68 W. This result outperforms the conventional cooking vessel by 25.4%. This achievement clearly demonstrates that the main factor influencing the performance at partial loads is the geometrical configuration of the vessel, that acts as a radiation receiver, as was explained in Section 2.3.

5. Conclusions and future research

This work analyses the influence of using a cooking vessel with partial loads on the performance of a funnel solar cooker. The main conclusions are:

1) Results from a total number of 48 experimental tests showed clearly that partial loads lead to significant reductions in cooker

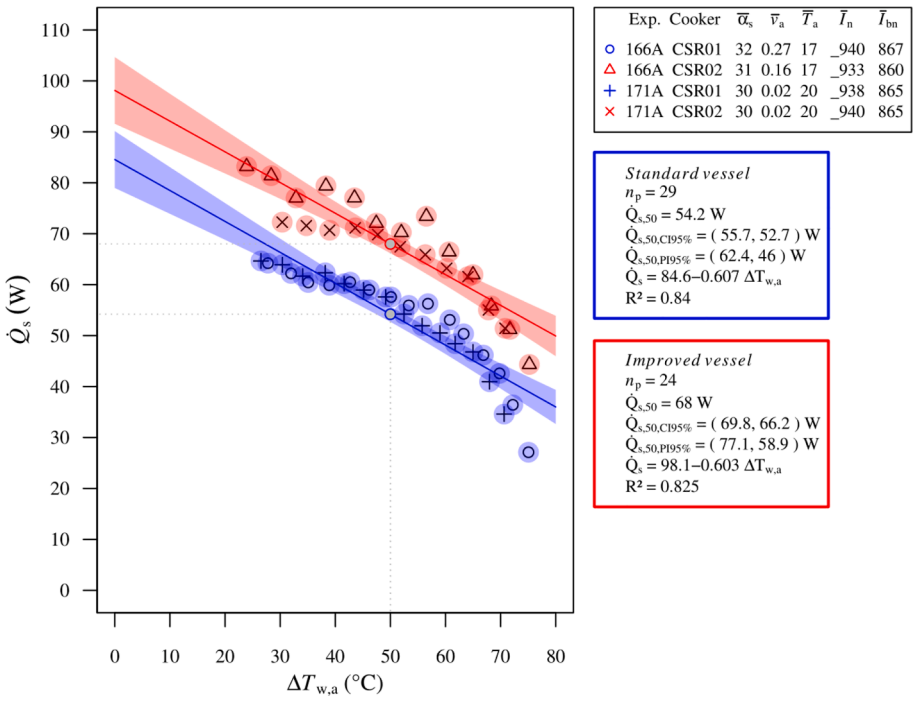

Fig. 15. Regression analysis of standard and improved cooking vessel, for 1.5 kg water load.

performance parameters in terms of both powers $\dot{Q}_{S,50}$ and $\dot{Q}_{S,0}$, because an under filled vessel receives proportionally more radiation on surfaces above the waterline (Section 3).

2) Simple correlations between the cooker powers $\dot{Q}_{S,50}$ and $\dot{Q}_{S,0}$ and the volumetric load fraction were derived, which are of interest to the practical user (Section 3).
3) Results also showed that the adoption of a glass enclosure increases the standardised power $\dot{Q}_{S,50}$ by about 30 to 40%, compared to the case without glass cover (Section 3).
4) A new design of cooking vessel, that improves cooker performance at partial loads was tested (Section 4). The standardized power obtained with the novel design outperform that obtained with the standard vessel by 25.4%, even if the same mass of water is adopted in both cooking vessel configuration.
5) ASAE S580.1 clustering time interval size of 10 min is not adequate for sampling fast tests (~40 min duration). A smaller 5 min interval has been found to be more suitable for both slow and fast tests, see Section 2.6.
6) It is recommended that a future version of the Standard should include testing at two different load levels, for example, at full load and at half load, in order to provide a more complete characterization of cooker performance under real-life operating conditions.

This work contributes to a better understanding of the factors that affect the thermal performance of solar cookers, investigating an aspect that has not been rigorously investigated before. Results are useful for practical users and also for developers of solar cookers that are looking to improve the vessel cooking design.

CRediT authorship contribution statement

Xabier Apaolaza-Pagoaga: Supervision, Conceptualization, Methodology, Formal analysis, Investigation, Data curation, Visualization, Writing – original draft, Writing – review & editing. **Antonio Carrillo-Andrés:** Conceptualization, Methodology, Formal analysis, Software, Investigation, Data curation, Visualization, Writing – original draft, Writing – review & editing. **Celestino Rodrigues Ruivo:** Conceptualization, Methodology, Formal analysis, Investigation, Writing – review & editing. **Francisco Fernández-Hernández:** Investigation, Writing – review & editing.

Declaration of Competing Interest

The authors declare that they have no known competing financial interests or personal relationships that could have appeared to influence the work reported in this paper.

Data availability

Data will be made available on request.

Appendix A. Experimental measured data

In present work, two sets of tests with a large number of experiments were carried out in Malaga, Spain, at a latitude of 36.9° N, and at an altitude of 57 m with 0.5, 1.0, 1.5 and 2 kg of water. One set of 31 experiments was carried out during 18 days for cooker operation with a glass enclosure and the other set of 15 experiments was carried out during 8 days for cooker operation without a glass enclosure. The experimental measured data for the tests using a glass enclosure are listed in Tables A1 to A4. The measured data during tests performed without a glass enclosure are listed in Tables A5 and A6. The Table A7 lists the measured data of another set of tests, which were conducted to investigate the influence of using an improved cooking vessel using glass enclosure and 1.5 kg of water. The recorded time indicated in all Tables A1 to A7 refers to solar time.

Table A1
Data of a first set of experiments carried out with a glass enclosure.

Expt. no.	107B	109B	110A	110A	110B	110B	110C	110C
Cooker	CSR1	CSR2	CSR1	CSR2	CSR1	CSR2	CSR1	CSR2
Start time	12:39	11:54	10:29	10:29	11:35	11:35	12:39	12:39
End time	13:23	12:36	11:06	11:05	12:09	12:08	13:14	13:13
Date	14 Jan 2021	29 Jan 2021	01 Feb 2021	01 Feb 2021	01 Feb 2021	01 Feb 2021	01 Feb 2021	01 Feb 2021
m_w(kg)	0.5	0.5	0.5	0.5	0.5	0.5	0.5	0.5
n_p	7	6	6	6	5	5	5	5
$\overline{I}_n$(W m^{-2})	982	960	966	966	974	974	987	987
$\overline{I}_{bn}$(W m^{-2})	914	895	889	889	896	896	900	900
$\overline{\alpha}_s$(°)	30	35	33	33	36	36	34	34
$\overline{T}_a$(°C)	18	26	21	21	22	22	23	23
$\overline{v}_a$(m s^{-1})	1.11	0.64	0.91	0.91	0.28	0.28	0.38	0.38
$\dot{Q}_{S,50}$(W)	43.7	52.7	48.7	50.1	53.2	55.3	50.3	52.4
$\dot{Q}_{S,0}$(W)	72.1	80.7	75.0	74.7	81.4	79.8	77.6	78.1
a(W °C^{-1})	−0.57	−0.56	−0.53	−0.49	−0.56	−0.49	−0.55	−0.52
R^2(-)	0.991	0.944	0.956	0.926	0.981	0.964	0.987	0.976

Table A2
Data of a second set of experiments carried out with a glass enclosure.

Expt. no.	114B	114B	114C	114C	56A	57A	58A	58A
Cooker	CSR1	CSR2	CSR1	CSR2	CSR1	CSR2	CSR1	CSR2
Start time	11:43	11:43	12:58	12:58	10:40	10:42	10:14	10:14
End time	12:23	12:23	13:35	13:35	12:19	12:42	12:13	12:03
Date	17 Feb 2021	17 Feb 2021	17 Feb 2021	17 Feb 2021	11 Dec 2019	07 Jan 2020	16 Jan 2020	16 Jan 2020
m_w(kg)	0.5	0.5	0.5	0.5	1.0	1.0	1.0	1.0
n_p	7	7	6	6	10	13	14	13
$\overline{I}_n$(W m^{-2})	888	888	951	951	964	936	946	946
$\overline{I}_{bn}$(W m^{-2})	731	731	806	806	876	856	856	858
$\overline{\alpha}_s$(°)	41	41	38	38	30	31	32	32
$\overline{T}_a$(°C)	18	18	21	21	21	17	18	18
$\overline{v}_a$(m s^{-1})	0.70	0.70	0.32	0.32	1.20	1.11	1.00	0.99
$\dot{Q}_{S,50}$(W)	49.5	50.7	50.8	51.4	53.2	53.9	50.3	55.7
$\dot{Q}_{S,0}$(W)	74.2	74.5	81.7	78.7	84.5	87.3	87.8	86.6
a(W °C^{-1})	−0.49	−0.48	−0.62	−0.55	−0.63	−0.67	−0.75	−0.62
R^2(-)	0.966	0.966	0.991	0.970	0.972	0.986	0.955	0.951

Table A3
Data of a third set of experiments carried out with a glass enclosure.

Expt. no.	105B	56A	57A	60A	60A	105B	44A	45A
Cooker	CSR1	CSR2	CSR1	CSR1	CSR2	CSR2	CSR2	CSR2
Start time	12:39	10:40	10:42	10:50	10:50	12:39	10:34	11:02
End time	13:59	12.54	12:57	12:40	12:40	13:59	12:13	12:41
Date	12 Jan 2021	11 Dec 2019	07 Jan 2020	27 Jan 2020	27 Jan 2020	12 Jan 2021	6 Nov 2019	12 Nov 2019
m_w(kg)	1.0	1.5	1.5	1.5	1.5	1.5	2.0	2.0
n_p	12	12	16	12	13	12	14	14
$\overline{I}_n$(W m^{-2})	940	971	939	927	929	940	968	961
$\overline{I}_{bn}$(W m^{-2})	873	883	858	840	842	873	874	874
$\overline{\alpha}_s$(°)	28	30	31	35	35	28	37	35
$\overline{T}_a$(°C)	16	22	17	19	19	16	20	20
$\overline{v}_a$(m s^{-1})	0.60	1.18	1.10	0.78	0.76	0.60	1.18	1.62
$\dot{Q}_{S,50}$(W)	53.0	57.4	57.6	72.3	72.9	56.8	75.3	72.8
$\dot{Q}_{S,0}$(W)	102.5	93.3	88.7	106.2	101.7	93.7	102.3	105.2
a(W °C^{-1})	−0.99	−0.72	−0.62	−0.68	−0.58	−0.74	−0.54	−0.65
R^2(-)	0.906	0.992	0.983	0.963	0.927	0.960	0.894	0.944

Table A4
Data of a fourth set of experiments carried out with a glass enclosure.

Expt. no.	46A	51A	52A	53A	63A	63A	64A	105A
Cooker	CSR2	CSR2	CSR2	CSR1	CSR1	CSR2	CSR2	CSR1
Start time	10:30	9:30	10:20	10:58	11:39	11:39	10:34	10:14
End time	12:28	11:49	12:19	12:47	13:28	13:28	12:03	12:05
Date	15 Nov 2019	28 Nov 2019	29 Nov 2019	04 Dec 2019	10 Feb 2020	10 Feb 2020	11 Feb 2020	12 Jan 2021
m_w(kg)	2.0	2.0	2.0	2.0	2.0	2.0	2.0	2.0
n_p	12	17	15	10	13	13	10	15
$\bar{I}_n$(W m^{-2})	982	919	948	996	976	976	982	975
$\bar{I}_{bn}$(W m^{-2})	840	830	883	836	877	877	879	915
$\bar{\alpha}_s$(°)	35	31	31	31	37	37	39	31
$\bar{T}_a$(°C)	15	22	23	20	22	22	23	15
$\bar{v}_a$(m s^{-1})	1.47	1.17	1.33	0.87	1.36	1.36	1.08	0.19
$\dot{Q}_{S,50}$(W)	71.0	68.6	74.9	68.9	78.6	78.2	82.7	77.4
$\dot{Q}_{S,0}$(W)	103.5	100.5	102.6	98.0	112.9	113.5	121.4	103.0
a(W °C^{-1})	−0.65	−0.64	−0.55	−0.58	−0.69	−0.71	−0.77	−0.51
R^2(-)	0.985	0.952	0.948	0.987	0.937	0.931	0.957	0.815

Table A5
Data of a first set of experiments carried out without a glass enclosure.

Expt. no.	106B	107B	108A	109B	114A	114A	111A	112A
Cooker	CSR1	CSR2	CSR2	CSR1	CSR1	CSR2	CSR2	CSR1
Start time	12:44	12:39	10:04	11:54	10:03	10:03	10:53	10:03
End time	14:04	13:59	11:15	12:36	11:08	11:06	12:16	11:23
Date	13 Jan 2021	14 Jan 2021	15 Jan 2021	29 Jan 2021	17 Feb 2021	17 Feb 2021	02 Feb 2021	11 Feb 2021
m_w(kg)	0.5	0.5	0.5	0.5	0.5	0.5	1.0	1.0
n_p	6	6	8	8	11	11	14	13
$\bar{I}_n$(W m^{-2})	966	983	955	960	848	848	1005	931
$\bar{I}_{bn}$(W m^{-2})	900	916	887	894	696	696	927	814
$\bar{\alpha}_s$(°)	30	30	29	35	37	37	36	36
$\bar{T}_a$(°C)	17	18	16	26	17	17	21	23
$\bar{v}_a$(m s^{-1})	0.27	1.11	0.38	0.57	0.19	0.19	1.01	0.48
$\dot{Q}_{S,50}$(W)	33.7	25.8	42.4	36.8	33.2	38.6	42.1	46.2
$\dot{Q}_{S,0}$(W)	79.8	75.5	69.8	87.4	80.6	84.8	89.4	87.2
a(W °C^{-1})	−0.92	−0.99	−0.77	−1.01	−0.95	−0.92	−0.95	−0.82
R^2(-)	0.994	0.991	0.958	0.981	0.990	0.986	0.993	0.976

Table A6
Data of a second set of experiments carried out without a glass enclosure.

Expt. no.	111A	111B	113A	113A	106A	107A	109A
Cooker	CSR1	CSR1	CSR1	CSR2	CSR1	CSR2	CSR1
Start time	10:53	12:44	12:48	12:48	10:04	10:04	10:00
End time	12:33	14:04	14:08	14:08	12:24	12:24	11:40
Date	02 Feb 2021	02 Feb 2021	15 Feb 2021	15 Feb 2021	13 Jan 2021	14 Jan 2021	29 Jan 2021
m_w(kg)	1.5	1.5	1.5	1.5	2.0	2.0	2.0
n_p	16	13	11	11	21	21	14
$\bar{I}_n$(W m^{-2})	1001	957	963	963	972	981	941
$\bar{I}_{bn}$(W m^{-2})	917	857	837	837	908	917	871
$\bar{\alpha}_s$(°)	36	32	35	35	31	31	33
$\bar{T}_a$(°C)	22	24	19	19	15	17	23
$\bar{v}_a$(m s^{-1})	0.95	0.76	1.02	1.02	0.23	0.97	0.41
$\dot{Q}_{S,50}$(W)	50.8	43.3	43.1	39.2	58.31	48.1	66.3
$\dot{Q}_{S,0}$(W)	97.5	99.6	107.8	104.8	99.9	96.4	94.5
a(W °C^{-1})	−0.93	−1.13	−1.29	−1.31	−0.83	−0.97	−0.56
R^2(-)	0.985	0.951	0.984	0.979	0.976	0.978	0.890

Table A7
Data of a recent set of experiments carried out with the standard pot and the modified pot.

Expt. no.	166A	166A	171A	171A
Cooker	CSR1	CSR2	CSR2	CSR1
Vessel	Standard	Improved	Standard	Improved
Start time	10:00	10:00	10:00	10:00
End time	12:00	12:00	12:00	12:00
Date	23 Nov 2021	23 Nov 2021	01 Dec 2021	01 Dec 2021
m_w(kg)	1.5	1.5	1.5	1.5
n_p	15	13	14	11
$\bar{I}_n$(W m^{-2})	940	933	938	940
$\bar{I}_{bn}$(W m^{-2})	867	860	865	865
$\bar{\alpha}_s$(°)	32	31	30	30
$\bar{T}_a$(°C)	17	17	20	20
$\bar{v}_a$(m s^{-1})	0.27	0.16	0.02	0.02
$\dot{Q}_{S,50}$(W)	54.5	69.5	54.0	66.2
$\dot{Q}_{S,0}$(W)	85.2	102.9	84.0	89.9
a(W °C^{-1})	−0.62	−0.67	−0.60	−0.47
R^2(-)	0.797	0.869	0.902	0.847

References

[1] World Health Organization (WHO). Indoor air pollution and health. http://www.who.int/mediacentre/factsheets/fs292/en/ (Accessed 1 April 2022).

[2] J.M.F. Mendoza, A. Gallego-Schmid, X.C. Schmidt Rivera, J. Rieradevall, A. Azapagic, Sustainability assessment of home-made solar cookers for use in developed countries, Sci. Total Environ., 648 (2019) 184–196, https://doi.org/10.1016/j.scitotenv.2018.08.125.

[3] Solar Cookers International (SCI). Classroom resources. https://solarcooking.fandom.com/wiki/Classroom_resources (Accessed 1 April 2022).

[4] Solar Education Project (SEP). https://gdsnonprofit.org/solar-education-project (Accessed 1 April 2022).

[5] GoSun Users discuss the best solar oven for a power outage. https://gosun.co/blogs/news/the-best-gosun-for-grid-failure (Accessed 1 April 2022).

[6] Solar Cookers International (SCI). The energy crisis on a global scale. http://solarcooking.org/globalenergycrisis.htm.

[7] M. Aramesh, M. Ghalebani, A. Kasaeian, H. Zamani, G. Lorenzini, O. Mahian, S. Wongwises, A review of recent advances in solar cooking technology, Renew. Energy 140 (2019) 419–435, https://doi.org/10.1016/j.renene.2019.03.021.

[8] U.C. Arunachala, A. Kundapur, Cost-effective solar cookers: A global review, Sol. Energy 207 (2020) 903–916, https://doi.org/10.1016/j.solener.2020.07.026.

[9] E. Cuce, P.M. Cuce, A comprehensive review on solar cookers, Appl. Energy 102 (2013) 1399–1421, https://doi.org/10.1016/j.apenergy.2012.09.002.

[10] A. Saxena, B. Norton, V. Goel, et al., Solar cooking innovations, their appropriateness, and viability, Environ. Sci. Pollut. Res. 29 (2022) 58537–58560, https://doi.org/10.1007/s11356-022-21670-4.

[11] E. González-Mora, E. A. Rincón-Mejía, Optical Evaluation of the Tolokatsin-2020 High-Efficiency Solar Cooker, ISES Solar World Congress 2021, virtual conference, 25-29 October 2021.

[12] I. Yaholnitsky, A parabolic trough baking device developed in Lesotho, Consolfood 2020, Faro-Portugal, 22-24 January, 2020.

[13] M. Hosseinzadeh, A. Faezian, S.M. Mirzababaee, H. Zamani, Parametric analysis and optimization of a portable evacuated tube solar cooker, Energy 194 (2020), 116816, https://doi.org/10.1016/j.energy.2019.116816.

[14] Solar Cookers International. Solar cooker designs. https://solarcooking.fandom.com/wiki/Category:Solar_cooker_designs (Accessed 1 April 2022).

[15] Solar Cookers International, Cookit Solar Cookers. Solar Cooking Wiki. https://solarcooking.fandom.com/wiki/CooKit / (Accessed 1 April 2022).

[16] S.M. Ebersviller, J.J. Jetter, Evaluation of performance of household solar cookers, Sol. Energy 208 (2020) 166–172, https://doi.org/10.1016/j.solener.2020.07.056.

[17] X. Apaolaza-Pagoaga, A. Carrillo-Andrés, C. Ruivo, Experimental characterization of the thermal performance of the Haines 2 solar cooker, Energy 257 (2022), 124730, https://doi.org/10.1016/j.energy.2022.124730.

[18] Haines Solar Cookers. https://hainessolarcookers.com/ (Accessed 1 April 2022).

[19] X. Apaolaza-Pagoaga, A. Carrillo-Andrés, C. Ruivo, Experimental thermal performance evaluation of different configurations of Copenhagen solar cooker, Renew. Energy 184 (2022) 604–618, https://doi.org/10.1016/j.renene.2021.11.105.

[20] C. Ruivo, A. Carrillo-Andrés, X. Apaolaza-Pagoaga, Experimental determination of the standardised power of a solar funnel cooker for low sun elevations, Renew. Energy 170 (2021) 364–374, https://doi.org/10.1016/j.renene.2021.01.146.

[21] X. Apaolaza-Pagoaga, A.A. Sagade, C. Rodrigues Ruivo, A. Carrillo-Andrés, Performance of solar funnel cookers using intermediate temperature test load under low sun elevation, Sol. Energy 225 (2021) 978–1000, https://doi.org/10.1016/j.solener.2021.08.006.

[22] X. Apaolaza-Pagoaga, A. Carrillo-Andrés, C. Ruivo, New approach for analysing the effect of minor and major solar cooker design changes: influence of height trivet on the power of a funnel cooker, Renew. Energy 179 (2021) 2071–2085, https://doi.org/10.1016/j.renene.2021.08.025.

[23] A. Carrillo-Andrés, X. Apaolaza-Pagoaga, C. Rodrigues Ruivo, E. Rodríguez-García, F. Fernández-Hernández, Optical characterization of a funnel solar cooker with azimuthal sun tracking through ray-tracing simulation, Sol. Energy 233 (2022) 84–95, https://doi.org/10.1016/j.solener.2021.12.027.

[24] S.C. Mullick, T.C. Kandpal, A.K. Saxena, Thermal test procedure for box type solar cooker, Sol. Energy 39 (1987) 353–360, https://doi.org/10.1016/S0038-092X(87)80021-X.

[25] P.J. Lahkar, R.K. Bhamu, S.K. Samdarshi, Enabling inter-cooker thermal performance comparison based on cooker opto-thermal ratio (COR), Appl. Energy 99 (2012) 491–495, https://doi.org/10.1016/j.apenergy.2012.05.034.

[26] P.A. Funk, Evaluating the international standard procedure for testing solar cookers and reporting performance, Sol. Energy 68 (2000) 1–7, https://doi.org/10.1016/S0038-092X(99)00059-6.

[27] ASAE S580.1 NOV2013, Testing and reporting solar cooker performance, American Society of Agricultural Engineers, Michigan, USA, 2013.

[28] A. Kumar, A. Saxena, S.D. Pandey, S.K. Joshi, Design and performance characteristics of a solar box cooker with phase change material: A feasibility study for Uttarakhand region, Appl. Therm. Eng. 208 (2022), 118196, https://doi.org/10.1016/j.applthermaleng.2022.118196.

[29] S.S. Ghosh, P.K. Biswas, S. Neogi, Thermal performance of solar cooker with special cover glass of low-e antimony doped indium oxide (IAO) coating, Appl. Therm. Eng. 113 (2017) 103–111, https://doi.org/10.1016/j.applthermaleng.2016.10.185.

[30] Ippon panel light datasheet. https://www.aalco.es/proyectos/ippon-panellight/ (Accessed 1 April 2022).

[31] C. Ruivo, X. Apaolaza-Pagoaga, A. Carrillo-Andrés, G. Coccia, Influence of the aperture area on the performance of a solar funnel cooker operating at high sun elevations using glycerine as load, Sustain. Energy Technol. Assess. 53 (2022), 102600, https://doi.org/10.1016/j.seta.2022.102600.

[32] J.A. Duffie, W.A. Beckman, Solar Engineering of Thermal Processes, fourth ed., Willey, 2013.

[33] C. Ruivo, X. Apaolaza-Pagoaga, G. Di Nicola, A. Carrillo-Andrés, On the use of experimental measured data to derive the linear regression usually adopted for determining the performance parameters of a solar cooker, Renew. Energy 181 (2021) 105–115, https://doi.org/10.1016/j.renene.2021.09.047.

[34] A.A. Sagade, X. Apaolaza-Pagoaga, C. Ruivo, A. Carrillo-Andrés, Concentrating solar cookers in urban areas: Establishing usefulness through realistic intermediate temperature rating and grading, Sol Energy 241 (2022) 157–166, https://doi.org/10.1016/j.solener.2022.06.007.

[35] S.C. Mullick, T.C. Kandpal, S. Kumar, Testing of box-type solar cooker: second figure of merit F2 and its variation with load and number of pots, Sol. Energy. 57 (1996) 409–413, https://doi.org/10.1016/S0038-092X(96)00116-8.

[36] P. Bruce, A. Bruce, Practical statistics for data scientists. First ed. O'Reilly Media, 2016.

[37] R Core Team, R: A Language and Environment for Statistical Computing. R Foundation for Statistical Computing (2019). https://www.R-project.org/.